
Res-Tuning: A Flexible and Efficient Tuning Paradigm via Unbinding Tuner from Backbone

Zeyinzi Jiang¹ Chaojie Mao¹ Ziyuan Huang² Ao Ma¹
 Yiliang Lv¹ Yujun Shen³ Deli Zhao¹ Jingren Zhou¹

¹Alibaba Group ²National University of Singapore ³Ant Group
 {zeyinzi.jzyz, chaojie.mcj, dave.ma, yiliang.lyl, jingren.zhou}@alibaba-inc.com
 {ziyuan.huang}@u.nus.edu {shenyujun0302, zhaodeli}@gmail.com

Abstract

Parameter-efficient tuning has become a trend in transferring large-scale foundation models to downstream applications. Existing methods typically *embed* some light-weight tuners into the backbone, where both the design and the learning of the tuners are highly dependent on the base model. This work offers a new tuning paradigm, dubbed Res-Tuning, which intentionally *unbinds* tuners from the backbone. With both theoretical and empirical evidence, we show that popular tuning approaches have their equivalent counterparts under our unbinding formulation, and hence can be integrated into our framework effortlessly. Thanks to the structural disentanglement, we manage to free the design of tuners from the network architecture, facilitating flexible combination of various tuning strategies. We further propose a memory-efficient variant of Res-Tuning, where the bypass (*i.e.*, formed by a sequence of tuners) is effectively detached from the main branch, such that the gradients are back-propagated only to the tuners but not to the backbone. Such a detachment also allows one-time backbone forward for multi-task inference. Extensive experiments on both discriminative and generative tasks demonstrate the superiority of our method over existing alternatives from the perspectives of efficacy and efficiency. Project page: <https://res-tuning.github.io/>.

1 Introduction

Recently, foundation models have demonstrated strong generalization capability across numerous visual [21, 2], language [47, 60] and multi-modal tasks [40, 1]. Pre-trained on a large corpus of data, a foundation model offers a good initialization for downstream adaptation. Unfortunately, the increasing model scale makes it expensive and almost infeasible to fully fine-tune such a model for every task. Hence, parameter-efficient transfer learning (PETL) [37, 41, 27] is often resorted to as an efficient approach for downstream adaptation without incurring an unaffordable computation burden.

Popular existing approaches for parameter-efficient tuning introduce additional tunable structures (which we term as *tuners*) to the pre-trained base model [37, 41, 27]. Compared to the fully-fine-tuned counterparts, the light-weight tuners significantly reduce the training cost while maintaining a competitive performance [32, 28]. However, the current designs of tuners are deeply coupled with their base structures, as shown in Fig. 1a, thus restricting the design flexibility and impeding the extension to new approaches. For example, prefix tuning [41] is embedded into the self-attention operation, and prompts [28, 85] could only be introduced at the beginning or between layers, *etc.*

In this work, we introduce Res-Tuning, a new tuning paradigm for flexible and efficient transfer learning. As in Fig. 1b, our Res-Tuning framework unbinds the tuners from the base model, such that it is possible to decouple both the design and the learning of the tuners from the base structure. Since

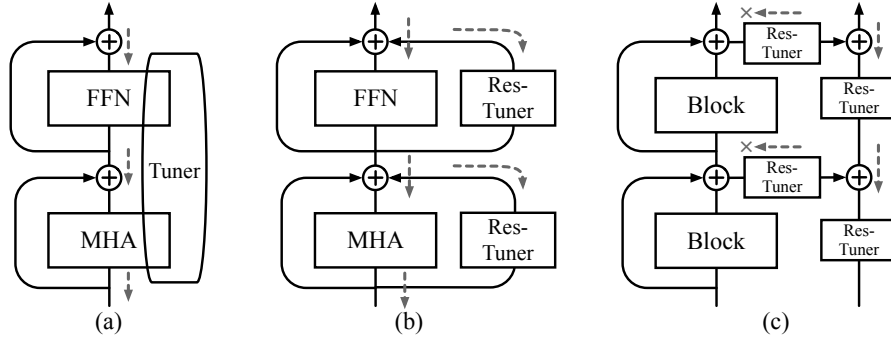


Figure 1: **Concept comparison** between existing methods and our Res-Tuning framework. (a) Existing PETL methods are deeply embedded into original structures. (b) Our Res-Tuning framework can decouple PETL methods from the backbone. (c) Backpropagation only through a bypass consisting of Res-Tuner can be achieved by detaching the connections.

the design of the tuners is no longer dependent on the base structure in our Res-Tuning framework, we explore various possibilities. With both theoretical and empirical evidence, we first show that our framework can seamlessly encompass popular tuning approaches such as prefix-tuning [41], prompt-tuning [28], and adapters [25]. Further, it is demonstrated that the structural disentanglement also allows for flexible combination of various tuners, leading to the discovery of stronger tuning strategies. On top of that, we show that such an unbinding formulation also allows for the detachment of the tuners from the backbone as in Fig. 1c, which further improves the memory efficiency. In this memory-efficient version, *i.e.*, Res-Tuning-Bypass, not only is the training cost reduced because the gradient computation through the massive parameters is avoided in the base model, but it also reduces the number of forward passes of the backbone model to only once during multi-task inference.

We evaluate Res-Tuning framework on both discriminative and generative tasks. On discriminative tasks, we show that our unbinding formulation leads to a tuning strategy that achieves state-of-the-art performance on VTAB-1K with similar learnable parameters. Our Res-Tuning-Bypass framework also performs favorably against the fully-fine-tuned variant, while reducing the training memory consumption by 49.7% and the multi-task inference time by 80.9%. In addition, it also obtains better performance in few-shot learning and domain generalization scenarios. On generative tasks, apart from the strong performance achieved by Res-Tuning framework in terms of both FID scores and qualitative results, we further show that our Res-Tuning-Bypass can reduce the memory consumption by 70.7%, training time by 58.6%, and multi-task inference time by 83.6% when maintaining a competitive FID score and generation quality compared to the fully-fine-tuned variant.

2 Unbinding parameter-efficient tuning

In order to reduce the entanglement between the base model and the tuners as well as to increase the flexibility of the tuning strategies, we set out to unbind the tuners from the pre-trained structures. In this section, we provide our unbinding formulation to existing parameter-efficient transfer learning strategies. We start by revisiting the basic building blocks of the foundation models, before diving into unbinding existing tuners from the backbone. In the last part of this section, we further provide empirical proof that our unbinding formulation could seamlessly encompass existing PETL methods like prompt tuning [28], prefix tuning [41], and adapters [25].

2.1 Basic building blocks of foundation models

Existing foundation models in both natural language processing, vision, and vision-language applications mostly adopt Transformers [70] as the backbone. The major building blocks of the Transformers that one usually adapts for the downstream tasks are the multi-head attention (MHA) and the feed-forward network (FFN). Formally, the standard MHA and FFN could be expressed as:

$$\text{Attn}(\mathbf{Q}, \mathbf{K}, \mathbf{V}) = \text{softmax}\left(\frac{\mathbf{Q}\mathbf{K}^T}{\sqrt{d}}\right)\mathbf{V}, \quad (1)$$

$$\text{FFN}(\mathbf{x}) = \phi(\mathbf{x}\mathbf{W}_1 + \mathbf{b}_1)\mathbf{W}_2 + \mathbf{b}_2$$

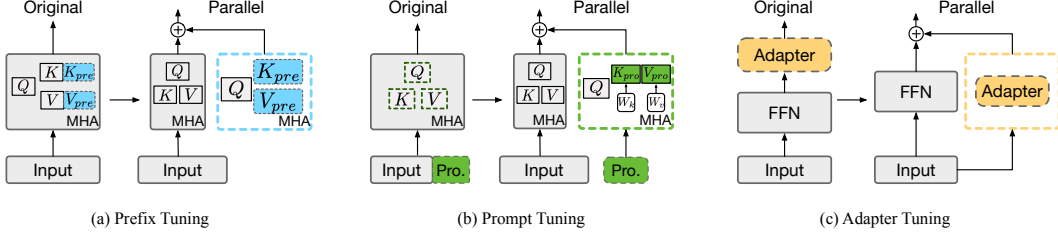


Figure 2: **The original and the unbinding form** of (a) prefix tuning [41], (b) prompt tuning [28], and (c) adapter tuning [25] for parameter-efficient transfer learning.

where Q , K and V denote the query, key and value, respectively. W_1 and W_2 are the projection weights, b_1 and b_2 are the bias terms, and ϕ is the non-linear activation between fully-connected layers. Usually, given input tokens x , the query, key, and value are obtained through a linear projection $Q = xW_q$, $K = xW_k$, and $V = xW_v$, where W_q , W_k and W_v are learnable projection weights.

2.2 Unbinding tuners from foundation models

For the adaptation of the foundation models to downstream applications, the existing PETL approaches mostly resort to adjusting the output of MHA, FFN, or the Transformer block composed of MHA and FFN in various ways. We choose popular and exemplary approaches and unbind their structures from foundation models. Here, we provide the unbinding formulations of prefix tuning [41] and prompt tuning [28] for MHA adaptation, as well as adapter tuning [25] for FFN adaptation.

Prefix tuning [41] prepends learnable parameters, *i.e.*, prefix tokens, to the projected keys and values:

$$\text{MHA}_{\text{pre}} = \text{Attn}(xW_q, [K_{\text{pre}}; xW_k], [V_{\text{pre}}; xW_v]), \quad (2)$$

where K_{pre} and V_{pre} are prefix tokens. Essentially, if we view this as performing MHA separately between (Q, K, V) and between $(Q, K_{\text{pre}}, V_{\text{pre}})$, we unbind prefix tuning as follows:

$$\text{MHA}_{\text{pre}} = (1 - \lambda) \underbrace{\text{Attn}(Q, K, V)}_{\text{original attention}} + \lambda \underbrace{\text{Attn}(Q, K_{\text{pre}}, V_{\text{pre}})}_{\text{prefix attention in parallel}}, \quad (3)$$

where λ weighs between the original and prefix attention. Detailed value for λ and the derivation process are included in appendix A. In this way, the original MHA in the foundation model $\text{Attn}(Q, K, V)$ and the prefix attention $\text{Attn}(Q, K_{\text{pre}}, V_{\text{pre}})$ can be computed independently. The unbinding formulation of prefix tuning can be seen in Fig. 2a.

Prompt tuning [28] appends latent tokens to the input token before performing MHA in the backbone:

$$\text{MHA}_{\text{pro}} = \text{Attn}([x; x_{\text{pro}}]W_q, [x; x_{\text{pro}}]W_k, [x; x_{\text{pro}}]W_v), \quad (4)$$

where x_{pro} are prompt tokens concatenated to the input token x in the first layer or between multiple layers. Similar to prefix tuning, the unbinding formulation of prompt tuning is as follows:

$$\text{MHA}_{\text{pro}} = [(1 - \lambda) \underbrace{\text{Attn}(Q, K, V)}_{\text{original attention}} + \lambda \underbrace{\text{Attn}(Q, K_{\text{pro}}, V_{\text{pro}})}_{\text{prompt attention in parallel}}; D], \quad (5)$$

where $K_{\text{pro}} = x_{\text{pro}}W_k$ and $V_{\text{pro}} = x_{\text{pro}}W_v$. D denotes disposable parts that would not affect the output of MHA, where $D = (1 - \beta) \text{Attn}(Q_{\text{pro}}, K_{\text{pro}}, V_{\text{pro}}) + \beta \text{Attn}(Q_{\text{pro}}, K, V)$. λ and β are individual weights. More details can be seen in appendix A. The unbinding formulation of prompt tuning can be seen in Fig. 2b.

Adapter tuning [25] typically inserts a multi-layer perceptron (MLP) after FFN. Since the MLP could be performed independently, we simply re-route the adapter and connect it in parallel to the FFN as in Fig. 2c. The resultant unbinding formulation of the adapters is as follows:

$$\text{FFN}_{\text{adapter}} = \underbrace{\text{FFN}(x)}_{\text{original module}} + \underbrace{\phi(\text{FFN}(x)W_{\text{down}})}_{\text{adapter module in parallel}}W_{\text{up}}, \quad (6)$$

where W_{down} and W_{up} denote the weights for the down- and up-projection layers, respectively.

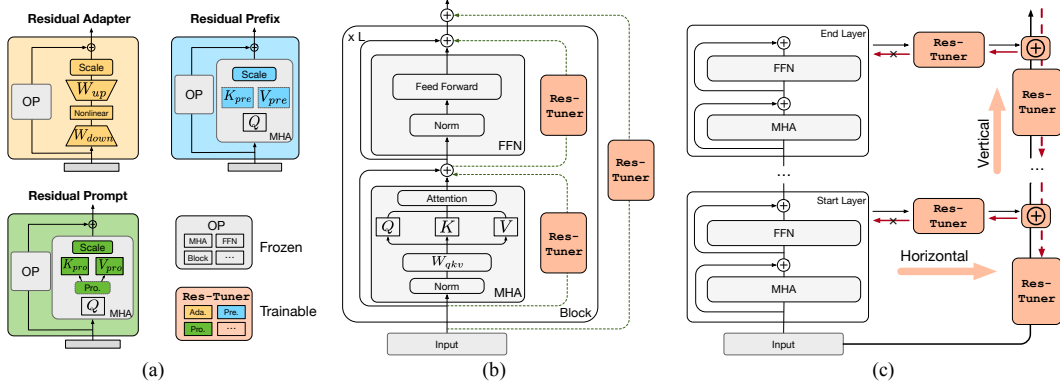


Figure 3: **Structure illustration** of (a) various Res-Tuners in our unbinding form, (b) our Res-Tuning framework that is flexible and efficient, and (c) Res-Tuning-Bypass, the memory-efficient version of our framework.

Table 1: **Empirical equivalence** of PETL methods and their counterparts in our unbinding form.

Method	ViT/B-16 (IN-21K)			ViT/L-14 (CLIP)		
	Original	Unbinding form	Δ	Original	Unbinding form	Δ
Adapter [25]	92.34	92.34	0.00	92.43	92.44	+0.01
Prefix [41]	91.90	91.88	-0.02	90.99	91.01	+0.02
Prompt [28]	92.21	92.24	+0.03	91.86	91.83	-0.03

2.3 Empirical equivalency of the unbinding formulation

After we have obtained the unbinding formulation of popular PETL methods with theoretical derivation, Tab. 1 shows empirical evidence of the equivalency between the original formulation and our unbinding formulation. We carry out the comparison between two formulations on CIFAR-100, using ViT [13] pre-trained on ImageNet-21K and by CLIP [59]. For all cases, we observe that the performance discrepancy between the original and our unbinding form is within a reasonable range (± 0.03), which shows that our formulation encompasses existing PETL methods effortlessly.

3 Res-Tuning

3.1 Unified formulation of Res-Tuning

Given the unbinding formulation of the existing PETL methods, we can derive a unified formulation as the combination of the frozen pre-trained operation and the tuner with learnable parameters:

$$\mathbf{x}' = \text{OP}(\mathbf{x}) + \text{Res-Tuner}(\mathbf{x}), \quad (7)$$

where OP denotes existing operations in the pre-trained backbone such as MHA and FFN, while the Res-Tuner represents the learnable structures that are connected in parallel to the existing operations.

With this unified unbinding formulation, the design of the tuner structure can now be independent of the original operation in the base model. This leads to unprecedented flexibility in parameter-efficient tuning, which enables us to explore various instantiations of the tuner (as in Fig. 3a) for the base structures. For example, we found in Tab. 2a that, instantiating the Res-Tuner with prompt tuning for FFN results in a better performance compared to adapters.

Further, the structural disentanglement also allows for the flexible combination of various tuning strategies. In Fig. 3b, we instantiate our Res-Tuning framework by associating one Res-Tuner with every operation in the base model, including MHA, FFN, and the whole Transformer block.

3.2 Res-Tuning-Bypass: Towards memory-efficient PETL

The unified formulation of Res-Tuning provides a viable solution for flexible and parameter-efficient transfer learning. However, since it is directly derived from existing PETL methods, it shares the

same vulnerability as existing PETL solutions. Despite the parameter efficiency, they require back-propagation through the massive parameters in the pre-trained backbone, which leads to unnecessary extra consumption of memory and computation.

To avoid this, we further present a memory-efficient version of our Res-Tuning framework, dubbed as Res-Tuning-Bypass, as in Fig. 3c. Specifically, we remove the data flow from the Res-Tuner to the backbone, such that the Res-Tuner is detached from the pre-trained architectures. In this way, we form a bypass network constructed by Res-Tuners in parallel with the backbone. Formally, given the tokenized feature x_0 and the output feature of the l -th layer x_l from the pre-trained model, our bypass network is formulated as:

$$\begin{aligned} x_0^{\text{bypass}} &= x_0, \\ x_l^{\text{bypass}} &= \lambda \text{Res-Tuner}(x_l) + (1 - \lambda) \text{Res-Tuner}(x_{l-1}^{\text{bypass}}), l \geq 1, \end{aligned} \tag{8}$$

where λ is a learnable parameter followed by a sigmoid function, which is initialized to 0.5. As demonstrated in Fig. 3c, we group the Res-Tuners in the bypass network into horizontal ones and vertical ones, respectively processing the output feature of the l -th layer from the backbone and the $(l - 1)$ -th feature from the bypass network. Within each group, we keep the structure identical. Thanks to the flexibility of our unbinding formulation, we can also explore different instantiations of the Res-Tuner and various combinations of the existing tuners.

4 Empirical evaluations on discriminative tasks

4.1 Experimental setups

Evaluation scenarios. We mainly analyze the flexibility and efficiency of our proposed Res-Tuning framework and evaluate the discriminative capabilities on three different scenarios: *transfer learning*, *few-shot learning*, and *domain generalization*.

Baselines. Apart from the traditional downstream adaptation methods like fully fine-tuning and linear probing, we divide existing tuning approaches into two categories: **(i)** methods focusing on parameter-efficiency, including adapter tuning [25], prefix tuning [41], VPT [28], LoRA [27], AdaptFormer [7], SSF [42], and NOAH[83]; **(ii)** methods focusing on memory-efficiency, including Side-Tuning [82], and LST [68]. Since these two categories have distinct characteristics with respect to the parameters, memory, and performance, we mainly compare our Res-Tuning framework within the former category, while the Res-Tuning-Bypass is mainly compared in the latter one.

Implementation details. For most experiments, we adopt ViT-B/16 [13] pre-trained on ImageNet-21K [11] as the backbone model, following VPT [28]. Unless otherwise specified, the middle of the adapter, as well as the number of prefix and prompt tokens in our Res-Tuning are set to 10 for parameter efficiency. We include the training details in appendix C. For all the tasks, we use top-1 accuracy as the main evaluation metric.

4.2 Analysis on flexibility

Flexible combination between backbone structures and tuners. Since our unbinding formulation allows for the structural disentanglement between the frozen structure in the backbone and the tuner with learnable parameters, it enables us to explore various combinations of the operation and the tuners. Here, we experiment with various instantiations of OP and Res-Tuner in our Res-Tuning framework, and the number of tuners is limited to one tuner per block (Single-Res-Tuner). The results are presented in Tab. 2a. We found that the default combination in existing approaches (prefix and prompt for MHA adaptation and adapter for FFN adaptation) is far from optimal, and connecting prompt tuning to FFN results in the best performance.

Flexible combination of multiple tuning strategies. Next, we show that the flexibility brought by our unbinding formulation could also effortlessly lead to stronger tuning strategies by combining various tuners in our unbinding formulation. Here, we consider two tuners per block (Dual-Res-Tuner), respectively connected to MHA and FFN. As in Tab. 2b, employing two tuners for each block brings notable improvements over the Single-Res-Tuner variants, with employing two adapters respectively for MHA and FFN achieving the strongest performance of 93.25. On top of the best performing Dual-Res-Tuner model, we further attach tuners at the block level in Tab. 2c. With

Table 2: **Exploration of various combinations** of operations in the pre-trained backbone and various Res-Tuners achieves a stronger performance compared to the existing tuning strategies on CIFAR-100. Adapter, prefix, and prompt are abbreviated as Ada., Pre. and Pro., respectively.

(a) Single-Res-Tuner .				(b) Dual-Res-Tuner .			(c) Tri-Res-Tuner .		
Tuner\OP	MHA	FFN	Block	MHA\FFN	Res-Ada.	Res-Pre.	Res-Pro.	Block	Dual-Res-Tuner
Res-Ada.	92.46	<u>92.34</u>	92.49	Res-Ada.	93.25	92.95	92.62	Res-Ada.	93.28
Res-Pre.	<u>91.88</u>	92.33	92.39	Res-Pre.	93.22	92.38	92.87	Res-Pre.	93.20
Res-Pro.	<u>92.24</u>	92.68	92.16	Res-Pro.	93.03	92.92	92.91	Res-Pro.	93.16

Table 3: **In-depth analysis** of our Res-Tuning and Res-Tuning-Bypass in terms of performance, parameter-efficiency and memory efficiency on CIFAR-100.

(a) Parameter efficiency of Res-Tuning on CIFAR-100.						(c) Performance and efficiency comparison with existing tuning strategies on CIFAR-100.			
Method	Full	Linear Probing	Single-	Dual-	Tri-	Method	Acc.	Param. (M)	Mem.
Acc.	89.12	85.95	92.68	93.25	93.28	Full	89.12	85.9 (100%)	9.02G
Param.	85.9M	0.07M	0.17M	0.48M	0.67M	Linear	85.95	0.07 (0.08%)	2.72G
(b) Parameter and memory efficiency of Res-Tuning-Bypass on CIFAR-100.						<i>Parameter-efficient tuning methods</i>			
Method	Bypass Res-Tuner	Acc.	Param.	Mem.		MAM-Adapter [†] [19]	91.70	10.08 (11.72%)	9.57G
Linear probing	✗ -	85.95	0.07M	2.72G	AdaptFormer [7]	91.86	1.26 (1.46%)	6.32G	
	✓ None	86.34	0.07M	3.48G	Res-Tuning	93.25	0.48 (0.55%)	6.85G	
	✓ Hori.	88.08	0.27M	3.66G	<i>Memory-efficient tuning methods</i>				
	✓ Vert.	87.26	0.27M	3.64G	Side-Tuning [82]	87.16	9.62 (11.18%)	3.48G	
Res-Tuning-Bypass	✓ Both	89.33	0.46M	4.72G	LST [†] [68]	88.72	0.93 (1.08%)	5.26G	
Fully fine-tuning	✗ -	89.12	85.9M	9.02G	Res-Tuning-Bypass	89.33	0.46 (0.53%)	4.72G	

[†] denotes our own implementation since the original approach is presented for natural language processing.

adapters on top of the Dual-Res-Tuner model, we observe further slight improvements on the classification performance. Compared to existing tuning strategies of underlining in Tab. 2a, without bells and whistles, the Tri-Res-Tuner version of our Res-Tuning framework achieves at least 0.94% performance improvement.

4.3 Analysis on parameter-, memory- and multi-task inference-efficiency

Parameter-efficiency. We analyze the parameter efficiency of our Res-Tuning framework in Tab. 3a. Our Single-Res-Tuner version surpasses the performance of the fully-fine-tuned variant with less than 0.2% learnable parameters. Combining all three tuners on MHA, FFN, and block-level, we manage to outperform the fully-fine-tuned and linear evaluated variants by respectively 4.16% and 7.33%, while only using 0.67M parameters.

Memory-efficiency. Here, we present the evolution from linear probing to our Res-Tuning-Bypass in Tab. 3b. It is observed that introducing a bypass network without any tuners can help ensemble the original features obtained from different layers, thereby mildly improving the classification accuracy as compared to the linear probing approach where only the classifiers are trained. On top of that, both horizontal and vertical Res-Tuner bring notable performance improvement with limited parameter and memory overhead. With both horizontal and vertical Res-Tuners in place, our Res-Tuning-Bypass framework achieves stronger performance with only 52% of the memory consumption when compared with the fully-fine-tuned variant.

Multi-task inference-efficiency. In Fig. 4, our Res-Tuning-Bypass demonstrates superior multi-task inference-efficiency on both discriminative and generative tasks. For discriminative multi-task inference, we combine the validation set of 19 tasks in VTAB-1K, perform 19 tasks on every image, and obtain the overall process time for the whole validation set. For generation multi-task inference, we take one image and provide the model with 10 fixed-length prompts for generation and record the overall generation time for the 10 prompts. For existing parameter-efficient methods, the inference time grows linearly when the number of tasks grows. Compared to the fully fine-tuned variant, all existing parameter-efficient tuning strategies increase the inference time to various extents. In contrast, our Res-Tuning-Bypass framework significantly reduces the inference time on 19 discriminative tasks and 10 generative tasks by respectively 80.9% and 83.6% when compared with the fully-fine-tuned variant.

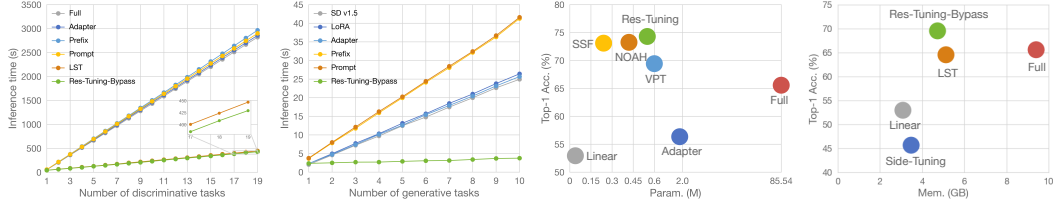


Figure 4: **Comparisons of the parameter-, memory-, and multi-task inference-efficiency.** For multi-task inference-efficiency, we evaluate Res-Tuning-Bypass on both discriminative and generative tasks. For parameter- and memory-efficiency, here, we show the comparisons on VTAB-1K between our approach and existing tuning strategies.

Table 4: **Performance and efficiency comparison** on the VTAB-1K benchmark with ViT-B/16 models pre-trained on ImageNet-21K. ‘‘Group Mean’’ denotes the average accuracy of the three subgroups. ‘‘All Mean’’ denotes the average accuracy of 19 downstream tasks.

	Natural						Specialized				Structured								Group Mean	All Mean	Param. (M)	Mem. (GB)	
	CIFAR-100	Caltech101	DTD	Flowers102	Pets	SVHN	Sun397	Camelyon	EuroSAT	Resisc45	Retinopathy	Clevr-Count	Clevr-Dist	DMLab	KITTI-Dist	dSpr-Loc	dSpr-Ori	sNORB-Azim	sNORB-Elev				
<i>Traditional methods</i>																							
Full	68.9	87.7	64.3	97.2	86.9	87.4	38.8	79.7	95.7	84.2	73.9	56.3	58.6	41.7	65.5	57.5	46.7	25.7	29.1	68.96	65.57	85.84	9.40
Linear	63.4	85.0	63.2	97.0	86.3	36.6	51.0	78.5	87.5	68.6	74.0	34.3	30.6	33.2	55.4	12.5	20.0	9.6	19.2	57.64	52.94	0.04	3.09
<i>Parameter-efficient tuning methods</i>																							
Adapter [25]	74.2	85.7	62.7	97.8	87.2	36.4	50.7	76.9	89.2	73.5	71.6	45.2	41.8	31.1	56.4	30.4	24.6	13.2	22.0	60.52	56.35	1.82	6.53
LoRA [27]	67.1	91.4	69.4	98.8	90.4	85.3	54.0	84.9	95.3	84.4	73.6	82.9	69.2	49.8	78.5	75.7	47.1	31.0	44.0	74.60	72.30	0.29	6.88
VPT-Deep [28]	78.8	90.8	65.8	98.0	88.3	78.1	49.6	81.8	96.1	83.4	68.4	68.5	60.0	46.5	72.8	73.6	47.9	32.9	37.8	71.96	69.43	0.60	8.13
SSF [42]	69.0	92.6	75.1	99.4	91.8	90.2	52.9	87.4	95.9	87.4	75.5	75.9	62.3	53.3	80.6	77.3	54.9	29.5	37.9	75.69	73.10	0.24	7.47
NOAH [83]	69.6	92.7	70.2	99.1	90.4	86.1	53.7	84.4	95.4	83.9	75.8	82.8	68.9	49.9	81.7	81.8	48.3	32.8	44.2	75.48	73.25	0.42	7.27
Res-Tuning	75.2	92.7	71.9	99.3	91.9	86.7	58.5	86.7	95.6	85.0	74.6	80.2	63.6	50.6	80.2	85.4	55.7	31.9	42.0	76.32	74.10	0.55	8.95
<i>Memory-efficient tuning methods</i>																							
Side-Tuning [82]	60.7	60.8	53.6	95.5	66.7	34.9	35.3	58.5	87.7	65.2	61.0	27.6	22.6	31.3	51.7	8.2	14.4	9.8	21.8	49.91	45.65	9.59	3.48
LST [†] [68]	58.0	87.1	66.2	99.1	89.7	63.2	52.6	81.9	92.2	78.5	69.4	68.6	56.1	38.8	73.4	72.9	30.5	16.6	31.0	67.56	64.52	0.89	5.13
Res-Tuning-Bypass	64.5	88.8	73.2	99.4	90.6	63.5	57.2	85.5	95.2	82.4	75.2	70.4	61.0	40.2	66.8	79.2	52.6	26.0	49.3	72.32	69.51	0.42	4.73

[†] denotes our own implementation since the original approach is proposed for natural language processing.

4.4 Comparisons with existing tuning strategies on different scenarios

Transfer Learning. We mainly evaluate our approach on the basic transfer learning scenario, where pre-trained models are fine-tuned on different downstream tasks. CIFAR-100 [35] is a standard general-purpose image classification dataset. VTAB-1K [80] is composed of 19 various visual classification tasks falling into three categorizations, *i.e.*, natural, specialized, and structured. We compare the performance of our approach and other baseline methods on the following:

CIFAR-100. We present the comparisons to existing tuning strategies in Tab. 3c. For parameter-efficient methods, our Res-Tuning framework notably improves over AdaptFormer [7] by 1.39%, using only 0.55% extra parameters, which is 0.91% less than AdaptFormer [7]. For memory-efficient methods, we outperform LST [68] by 0.61% with memory reduced by 0.54G (10%).

VTAB-1K. In Tab. 4, we present comprehensive evaluation on the 19 datasets on the VTAB-1K benchmark. Both our Res-Tuning and Res-Tuning-Bypass outperform existing approaches respectively within the group of parameter- and memory-efficient tuning methods. Specifically, our Res-Tuning framework achieves a 0.85% improvement in terms of the average performance on 19 datasets, compared to the previous best performance. For our Res-Tuning-Bypass, we outperform LST [68] in 18 out of 19 tasks and overall by 4.99% in terms of average performance. This is achieved with even fewer parameters and memory consumption. We further visualize the parameter vs. performance curve and memory vs. performance curve in Fig. 4 to show the advantage of our Res-Tuning and Res-Tuning-Bypass framework on VTAB-1K.

Few-Shot Learning. To evaluate the ability of our approach to adapt with only a few training samples, we follow the few-shot evaluation protocol in NOAH [83], using {1, 2, 4, 8, 16}-shots for training and full test data. We conduct experiments on five fine-grained datasets, including FGVC-Aircraft [51], Food-101 [4], Oxford Flowers [55], Oxford Pets [56], Stanford Cars [15].

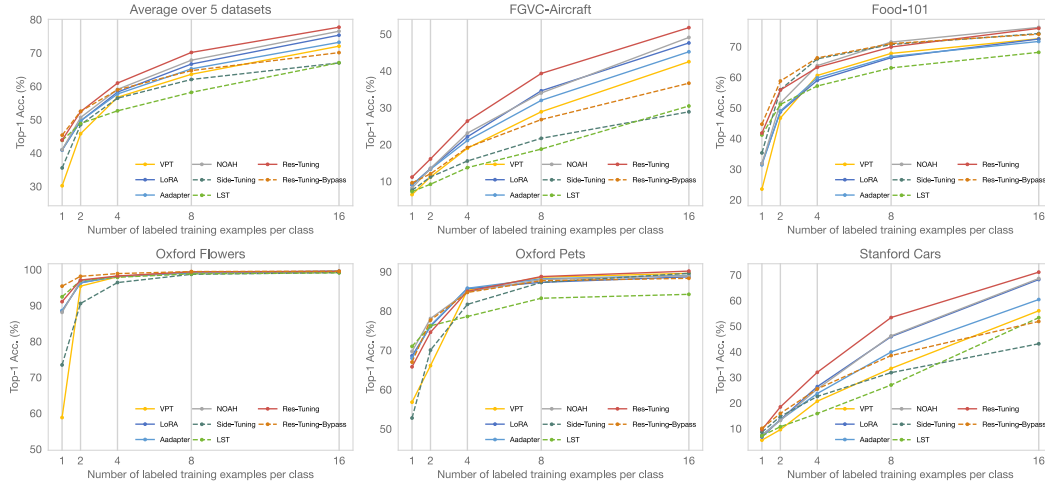


Figure 5: **Results of few-shot learning on five fine-grained visual recognition datasets.** The solid line represents the comparison of parameter-efficient tuning methods, and the dashed line represents the comparison of memory-efficient tuning methods. All results are averaged over 3 random seeds.

Table 5: **Results on domain generalization.** “Mean” denotes the average accuracy of four variants of ImageNet. All results are averaged over 3 random seeds.

	Source	Target				Mean
	ImageNet	IN-V2	IN-Sketch	IN-A	IN-R	
<i>Parameter-efficient tuning methods</i>						
Adapter [25]	70.5	59.1	16.4	5.5	22.1	25.8
VPT [28]	70.5	58.0	18.3	4.6	23.2	26.0
LoRA [27]	70.8	59.3	20.0	6.9	23.3	27.4
NOAH [83]	71.5	66.1	24.8	11.9	28.5	32.8
Res-Tuning	78.04	66.58	29.23	13.15	29.01	34.50
<i>Memory-efficient tuning methods</i>						
Side-Tuning [82]	74.57	62.52	23.55	10.37	25.06	30.38
LST [68]	70.00	57.04	14.39	7.21	17.02	23.92
Res-Tuning-Bypass	77.30	65.23	27.39	10.66	26.45	32.43

As the results are shown in Fig. 5, in terms of the overall performance (top-left), both Res-Tuning and Res-Tuning-Bypass demonstrate clear advantages over other corresponding parameter-efficient and memory-efficient tuning strategies of few-shot learning on five FGVC datasets. We also observe that Res-Tuning-Bypass performs as well as or even better than the non-memory-efficient methods on one or two shots with low training samples on several datasets.

Domain Generalization. To evaluate the robustness of our approach to distribution shift, we train a model on the source domain using 16 shots per category and test it on both the source and target domain. The source domain uses ImageNet-1K [11]) and the target domains use four other variants of ImageNet, including ImageNet-V2 [62], ImageNet-Sketch [73], ImageNet-A [24], ImageNet-R [23]. The results in Tab. 5 prove that our approach is robust under domain shift. Our Res-Tuning goes beyond NOAH [83] by 6.54% on ImageNet and 1.7% on the average accuracy of four variants of ImageNet. Furthermore, Res-Tuning-Bypass also demonstrates stronger robustness than the memory-efficient baselines and outperforms most existing parameter-efficient tuning methods.

5 Empirical evaluations on generative task

5.1 Experimental setups

Downstream tasks. To provide a more comprehensive evaluation of our Res-Tuning framework, we further apply it to the text-to-image generation task. Following [63], we evaluate the text-to-image

Table 6: **Comparison of FID and efficiency on COCO2017.** Following the default settings of stable diffusion¹, we sample 10k captions from the validation set for generating images of size 512² using 50 PLMS steps with classifier-free guidance scale 3.0 and compare against the full validation set.

Method	FID	Param. (M)	Mem. (GB)	Train (Hour/Epoch)
SD v1.5	15.48	-	-	-
+ Full	14.85	862 (100%)	72.77	1.98
+ LoRA	14.50	9.96 (1.15%)	61.03	1.42
+ Adapter	14.73	2.51 (0.29%)	54.30	1.30
+ Prefix	15.36	4.99 (0.58%)	64.91	2.20
+ Prompt	14.90	1.25 (0.14%)	63.70	2.17
+ Res-Tuning	13.96	2.54 (0.29%)	54.49	1.38
+ Res-Tuning Bypass	14.89	3.76 (0.44%)	21.35	0.82



Figure 6: **Qualitative results** of SD v1.5, existing tuning strategies and our Res-Tuning on COCO2017 validation set [43]. We frame our results in green and others in red.

generation performance on COCO2017 dataset [43]. The main quantitative evaluation metric is the FID score and we also perform instance-level fine-tuning transfer on the fine-grained datasets [4, 55].

Baselines. We experiment with the version 1.5 of stable diffusion [63] (SD) model. On COCO2017, we compare our Res-Tuning framework with zero-shot SD, SD with fully fine-tuning as well as SD with other existing tuning methods. On the fine-grained datasets, we employ DreamBooth [65] as our baseline and employ various tuning methods including our own for comparison.

5.2 Main results

Text-to-image generation on COCO. We show the comparison between our Res-Tuning framework and other approaches both quantitatively and qualitatively. The quantitative comparison is presented in Tab. 6. Compared with the fully fine-tuned baseline, our Res-Tuning framework improves the FID score by 0.89, using only 0.29% of the parameters. It is noteworthy that our Res-Tuning framework is the only approach that reaches a FID score below 14, while the best existing tuning strategy on the task is LoRA [27] achieving 14.50 with 4x the number of parameters in Res-Tuning. Hence, employing Res-Tuning could greatly facilitate the adaptation of pre-trained text-to-image generation models to downstream tasks.

A highlight is observed that our Res-Tuning-Bypass framework reduces the memory consumption for tuning the SD v1.5 model to only 29% while maintaining a similar performance (14.89 vs 14.85). Meanwhile, the time consumption for training the model is reduced to 41%. In terms of the reduction in the memory and time consumption, our Res-Tuning-Bypass framework outperforms the best tuning strategy by 3.3x (70.7% memory reduction of Res-Tuning-Bypass vs. 25.3% that of adapter) and 1.7x (58.6% reduction in time consumption of Res-Tuning-Bypass vs. 34.3% that of adapter), respectively.

The qualitative results are presented in Fig. 6. Both Res-Tuning and Res-Tuning-Bypass show a better alignment between the text and the generated image, where the surfboard is propped up in our generated images. Res-Tuning also demonstrates a better fidelity where the feather texture is realistic in the generated black bird.

¹<https://huggingface.co/runwayml/stable-diffusion-v1-5>

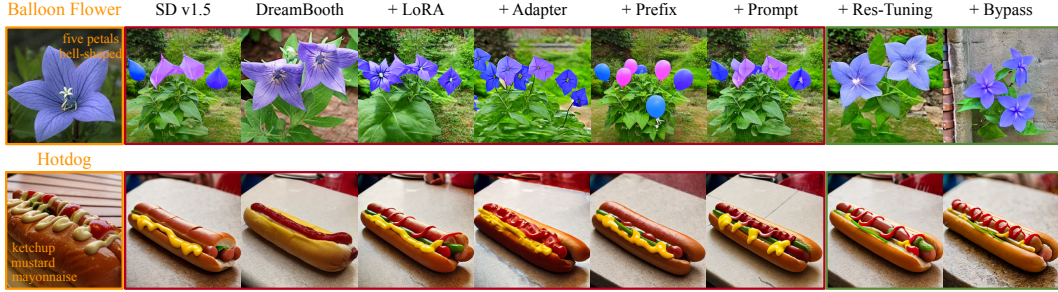


Figure 7: **Qualitative results** of SD v1.5, DreamBooth, existing tuning strategies, and our Res-Tuning on Oxford Flowers and Food-101 fine-grained dataset with the same generated seed. We frame our results in green and others in red.

Text-to-image generation on Oxford Flowers and Food-101. Here, we evaluate the transfer ability of existing tuning strategies on specific fine-grained categories. During every evaluation process, we select data from one specific category to train the model. The qualitative results are demonstrated in Fig. 7. It is observed that Res-Tuning presents a better view in terms of fidelity and the correct understanding of ambiguous categories. For example, the balloon flower is bell-shaped and has five petals, while existing approaches generate flowers with the wrong number of petals or even balloons rather than real flowers. Instead, both our Res-Tuning and our Res-Tuning-Bypass retain correct semantics and fine-grained features.

6 Related work

Transformers in computer vision. Transformers [70] have demonstrated strong capabilities in various fields [5, 61, 12, 59, 2, 17, 48, 53]. In computer vision, Vision Transformers (ViT) [13] are widely applied in various applications, such as visual classification [48, 39], object detection [67, 6], segmentation [84, 74] and generation [63, 57]. Owing to the strong scalability of the Transformer backbone [31, 10], recent endeavors either focus on expanding the size of the ViT [81] or training on a larger corpus of data in an unsupervised manner [75, 14].

Parameter-efficient tuning. Despite the strong performance and generalization ability brought by scaling up the Transformers, it also makes the adaptation to the downstream tasks expensive and almost infeasible. Hence, parameter-efficient transfer learning (PETL) emerged [26, 25, 76, 41, 85, 28]. Existing PETL methods could be generally categorized into three types: (i) MHA-based tuning embeds tunable parameters in the multi-head self-attention layers [27, 76, 28, 41, 45, 46]. (ii) FFN-based tuning methods represented by adapters [25] and its generalized versions [58, 33, 32, 19] introduce a multi-layer perceptron to the FFN layer. (iii) Other tuning methods adapt certain existing parameters [79, 42]. Closely related to our work, some recent efforts are devoted to finding out the optimal design paradigm of the tuning modules by neural architecture search [83]. Instead, we show that through our Res-Tuning framework, a stronger tuning strategy can be easily found by the flexible combination of several existing tuning strategies in our unbinding form.

Memory-efficient tuning. Since the structures of the existing PETL methods are deeply embedded in the backbone structure, back-propagation is required through the massive parameters of the pre-trained models, leading to unnecessary extra consumption of memory and computation. Hence, Side-Tuning [82] and LST [68] in natural language processing connect a side network in parallel with the pre-trained model to avoid data flow from the trainable parameters to the frozen ones. Our Res-Tuning-Bypass is inspired by the conceptual idea of these approaches. Compared to Side-Tuning and LST, we show that our Res-Tuning-Bypass is more flexible and memory-efficient.

7 Conclusion

In this work, we unbind the tuners from the backbone and form a flexible and efficient tuning paradigm Res-Tuning. With Res-Tuning, we are able to find stronger tuning strategies compared to existing ones. On top of Res-Tuning, we further extend a memory-efficient Res-Tuning-Bypass, which significantly reduces the memory consumption and multi-task inference cost. We hope our discoveries can facilitate further research in the flexible and efficient tuning of large foundation models.

References

- [1] J.-B. Alayrac, J. Donahue, P. Luc, A. Miech, I. Barr, Y. Hasson, K. Lenc, A. Mensch, K. Millican, M. Reynolds, et al. Flamingo: A visual language model for few-shot learning. *arXiv preprint arXiv:2204.14198*, 2022.
- [2] H. Bao, L. Dong, S. Piao, and F. Wei. BEiT: BERT pre-training of image Transformers. *arXiv preprint arXiv:2106.08254*, 2021.
- [3] C. Beattie, J. Z. Leibo, D. Teplyashin, T. Ward, M. Wainwright, H. Küttler, A. Lefrancq, S. Green, V. Valdés, A. Sadik, et al. Deepmind lab. *arXiv preprint arXiv:1612.03801*, 2016.
- [4] L. Bossard, M. Guillaumin, and L. Van Gool. Food-101 – mining discriminative components with random forests. In *Eur. Conf. Comput. Vis.*, 2014.
- [5] T. Brown, B. Mann, N. Ryder, M. Subbiah, J. D. Kaplan, P. Dhariwal, A. Neelakantan, P. Shyam, G. Sastry, A. Askell, et al. Language models are few-shot learners. In *Adv. Neural Inform. Process. Syst.*, 2020.
- [6] N. Carion, F. Massa, G. Synnaeve, N. Usunier, A. Kirillov, and S. Zagoruyko. End-to-end object detection with Transformers. In *Eur. Conf. Comput. Vis.*, pages 213–229, 2020.
- [7] S. Chen, C. Ge, Z. Tong, J. Wang, Y. Song, J. Wang, and P. Luo. AdaptFormer: Adapting vision Transformers for scalable visual recognition. In *Adv. Neural Inform. Process. Syst.*, 2022.
- [8] G. Cheng, J. Han, and X. Lu. Remote sensing image scene classification: Benchmark and state of the art. *Proceedings of the IEEE*, 2017.
- [9] M. Cimpoi, S. Maji, I. Kokkinos, S. Mohamed, , and A. Vedaldi. Describing textures in the wild. In *IEEE Conf. Comput. Vis. Pattern Recog.*, 2014.
- [10] M. Dehghani, J. Djolonga, B. Mustafa, P. Padlewski, J. Heek, J. Gilmer, A. Steiner, M. Caron, R. Geirhos, I. Alabdulmohsin, et al. Scaling Vision Transformers to 22 billion parameters. *arXiv preprint arXiv:2302.05442*, 2023.
- [11] J. Deng, W. Dong, R. Socher, L.-J. Li, K. Li, and L. Fei-Fei. ImageNet: A large-scale hierarchical image database. In *IEEE Conf. Comput. Vis. Pattern Recog.*, pages 248–255, 2009.
- [12] J. Devlin, M.-W. Chang, K. Lee, and K. Toutanova. BERT: Pre-training of deep bidirectional Transformers for language understanding. *North Am. Chap. Assoc. Comput. Linguist.*, 2018.
- [13] A. Dosovitskiy, L. Beyer, A. Kolesnikov, D. Weissenborn, X. Zhai, T. Unterthiner, M. Dehghani, M. Minderer, G. Heigold, S. Gelly, et al. An image is worth 16x16 words: Transformers for image recognition at scale. In *Int. Conf. Learn. Represent.*, 2020.
- [14] Y. Fang, W. Wang, B. Xie, Q. Sun, L. Wu, X. Wang, T. Huang, X. Wang, and Y. Cao. Eva: Exploring the limits of masked visual representation learning at scale. *arXiv preprint arXiv:2211.07636*, 2022.
- [15] T. Gebru, J. Krause, Y. Wang, D. Chen, J. Deng, and L. Fei-Fei. Fine-grained car detection for visual census estimation. In *Assoc. Adv. Artif. Intell.*, 2017.
- [16] A. Geiger, P. Lenz, C. Stiller, and R. Urtasun. Vision meets robotics: The KITTI dataset. *Int. J. Robotics Research*, 2013.
- [17] Y. Gong, Y.-A. Chung, and J. Glass. Ast: Audio spectrogram transformer. *arXiv preprint arXiv:2104.01778*, 2021.
- [18] B. Graham. Kaggle diabetic retinopathy detection competition report., 2015.
- [19] J. He, C. Zhou, X. Ma, T. Berg-Kirkpatrick, and G. Neubig. Towards a unified view of parameter-efficient transfer learning. In *Int. Conf. Learn. Represent.*, 2022.
- [20] K. He, X. Zhang, S. Ren, and J. Sun. Deep residual learning for image recognition. In *IEEE Conf. Comput. Vis. Pattern Recog.*, pages 770–778, 2016.
- [21] K. He, X. Chen, S. Xie, Y. Li, P. Dollár, and R. Girshick. Masked autoencoders are scalable vision learners. In *IEEE Conf. Comput. Vis. Pattern Recog.*, pages 16000–16009, 2022.
- [22] P. Helber, B. Bischke, A. Dengel, and D. Borth. Eurosat: A novel dataset and deep learning benchmark for land use and land cover classification. *IEEE Journal of Selected Topics in Applied Earth Observations and Remote Sensing*, 2019.

- [23] D. Hendrycks, S. Basart, N. Mu, S. Kadavath, F. Wang, E. Dorundo, R. Desai, T. Zhu, S. Parajuli, M. Guo, D. Song, J. Steinhardt, and J. Gilmer. The many faces of robustness: A critical analysis of out-of-distribution generalization. In *Int. Conf. Comput. Vis.*, 2021.
- [24] D. Hendrycks, K. Zhao, S. Basart, J. Steinhardt, and D. Song. Natural adversarial examples. In *IEEE Conf. Comput. Vis. Pattern Recog.*, 2021.
- [25] N. Houlsby, A. Giurgiu, S. Jastrzebski, B. Morrone, Q. De Laroussilhe, A. Gesmundo, M. Attariyan, and S. Gelly. Parameter-efficient transfer learning for NLP. In *Int. Conf. Mach. Learn.*, pages 2790–2799, 2019.
- [26] N. Houlsby, A. Giurgiu, S. Jastrzebski, B. Morrone, Q. De Laroussilhe, A. Gesmundo, M. Attariyan, and S. Gelly. Parameter-efficient transfer learning for nlp. In *Int. Conf. Mach. Learn.*, pages 2790–2799, 2019.
- [27] E. Hu, Y. Shen, P. Wallis, Z. Allen-Zhu, Y. Li, L. Wang, and W. Chen. LoRA: Low-rank adaptation of large language models. In *Int. Conf. Learn. Represent.*, 2021.
- [28] M. Jia, L. Tang, B.-C. Chen, C. Cardie, S. Belongie, B. Hariharan, and S.-N. Lim. Visual prompt tuning. In *Eur. Conf. Comput. Vis.*, 2022.
- [29] S. Jie and Z.-H. Deng. Convolutional bypasses are better vision Transformer adapters. *arXiv preprint arXiv:2207.07039*, 2022.
- [30] J. Johnson, B. Hariharan, L. van der Maaten, L. Fei-Fei, C. Lawrence Zitnick, and R. Girshick. Clevr: A diagnostic dataset for compositional language and elementary visual reasoning. In *IEEE Conf. Comput. Vis. Pattern Recog.*, 2017.
- [31] J. Kaplan, S. McCandlish, T. Henighan, T. B. Brown, B. Chess, R. Child, S. Gray, A. Radford, J. Wu, and D. Amodei. Scaling laws for neural language models. *arXiv preprint arXiv:2001.08361*, 2020.
- [32] R. Karimi Mahabadi, J. Henderson, and S. Ruder. Compacter: Efficient low-rank hypercomplex adapter layers. In *Adv. Neural Inform. Process. Syst.*, volume 34, pages 1022–1035, 2021.
- [33] R. Karimi Mahabadi, S. Ruder, M. Dehghani, and J. Henderson. Parameter-efficient multi-task fine-tuning for Transformers via shared hypernetworks. In *Assoc. Comput. Linguist.*, pages 565–576, 2021.
- [34] A. Khosla, N. Jayadevaprakash, B. Yao, and F.-F. Li. Novel dataset for fine-grained image categorization: Stanford dogs. In *IEEE Conf. Comput. Vis. Pattern Recog. Worksh.*, 2011.
- [35] A. Krizhevsky, G. Hinton, et al. Learning multiple layers of features from tiny images. *Master’s thesis, Department of Computer Science, University of Toronto*, 2009.
- [36] Y. LeCun, F. J. Huang, and L. Bottou. Learning methods for generic object recognition with invariance to pose and lighting. In *IEEE Conf. Comput. Vis. Pattern Recog.*, 2004.
- [37] B. Lester, R. Al-Rfou, and N. Constant. The power of scale for parameter-efficient prompt tuning. In *Conf. Empirical Methods NLP*, 2021.
- [38] F.-F. Li, R. Fergus, and P. Perona. One-shot learning of object categories. *IEEE Trans. Pattern Anal. Mach. Intell.*, 2006.
- [39] K. Li, Y. Wang, P. Gao, G. Song, Y. Liu, H. Li, and Y. Qiao. UniFormer: Unified Transformer for efficient spatiotemporal representation learning. In *Int. Conf. Learn. Represent.*, 2022.
- [40] L. H. Li, M. Yatskar, D. Yin, C.-J. Hsieh, and K.-W. Chang. VisualBERT: A simple and performant baseline for vision and language. *arXiv preprint arXiv:1908.03557*, 2019.
- [41] X. L. Li and P. Liang. Prefix-tuning: Optimizing continuous prompts for generation. In *Assoc. Comput. Linguist.*, pages 4582–4597, 2021.
- [42] D. Lian, D. Zhou, J. Feng, and X. Wang. Scaling & shifting your features: A new baseline for efficient model tuning. In *Adv. Neural Inform. Process. Syst.*, 2022.
- [43] T.-Y. Lin, M. Maire, S. Belongie, J. Hays, P. Perona, D. Ramanan, P. Dollár, and C. L. Zitnick. Microsoft COCO: Common objects in context. In *Eur. Conf. Comput. Vis.*, pages 740–755, 2014.
- [44] L. Liu, Y. Ren, Z. Lin, and Z. Zhao. Pseudo numerical methods for diffusion models on manifolds. In *Int. Conf. Learn. Represent.*, 2022.

- [45] X. Liu, K. Ji, Y. Fu, Z. Du, Z. Yang, and J. Tang. P-tuning v2: Prompt tuning can be comparable to fine-tuning universally across scales and tasks. *arXiv preprint arXiv:2110.07602*, 2021.
- [46] X. Liu, Y. Zheng, Z. Du, M. Ding, Y. Qian, Z. Yang, and J. Tang. GPT understands, too. *arXiv preprint arXiv:2103.10385*, 2021.
- [47] Y. Liu, M. Ott, N. Goyal, J. Du, M. Joshi, D. Chen, O. Levy, M. Lewis, L. Zettlemoyer, and V. Stoyanov. RoBERTa: A robustly optimized BERT pretraining approach. *arXiv preprint arXiv:1907.11692*, 2019.
- [48] Z. Liu, Y. Lin, Y. Cao, H. Hu, Y. Wei, Z. Zhang, S. Lin, and B. Guo. Swin Transformer: Hierarchical Vision Transformer using shifted windows. In *Int. Conf. Comput. Vis.*, 2021.
- [49] Z. Liu, H. Mao, C.-Y. Wu, C. Feichtenhofer, T. Darrell, and S. Xie. A convnet for the 2020s. In *IEEE Conf. Comput. Vis. Pattern Recog.*, pages 11976–11986, 2022.
- [50] I. Loshchilov and F. Hutter. Decoupled weight decay regularization. In *Int. Conf. Learn. Represent.*, 2019.
- [51] S. Maji, J. Kannala, E. Rahtu, M. Blaschko, and A. Vedaldi. Fine-grained visual classification of aircraft. *arXiv preprint arXiv:1306.5151*, 2013.
- [52] L. Matthey, I. Higgins, D. Hassabis, and A. Lerchner. dSprites: Disentanglement testing sprites dataset, 2017.
- [53] T. Meinhardt, A. Kirillov, L. Leal-Taixe, and C. Feichtenhofer. Trackformer: Multi-object tracking with transformers. In *IEEE Conf. Comput. Vis. Pattern Recog.*, pages 8844–8854, 2022.
- [54] Y. Netzer, T. Wang, A. Coates, A. Bissacco, B. Wu, and A. Y. Ng. Reading digits in natural images with unsupervised feature learning. In *Adv. Neural Inform. Process. Syst. Worksh.*, 2011.
- [55] M.-E. Nilsback and A. Zisserman. Automated flower classification over a large number of classes. In *Int. Conf. Comput. Vis. Graph. Image Process.*, pages 722–729, 2008.
- [56] O. M. Parkhi, A. Vedaldi, A. Zisserman, and C. V. Jawahar. Cats and dogs. In *IEEE Conf. Comput. Vis. Pattern Recog.*, 2012.
- [57] W. Peebles and S. Xie. Scalable diffusion models with Transformers. *arXiv preprint arXiv:2212.09748*, 2022.
- [58] J. Pfeiffer, A. Kamath, A. Rücklé, K. Cho, and I. Gurevych. AdapterFusion: Non-destructive task composition for transfer learning. In *Eur. Chap. Assoc. Comput. Linguist.*, pages 487–503, 2020.
- [59] A. Radford, J. W. Kim, C. Hallacy, A. Ramesh, G. Goh, S. Agarwal, G. Sastry, A. Askell, P. Mishkin, J. Clark, et al. Learning transferable visual models from natural language supervision. In *Int. Conf. Mach. Learn.*, pages 8748–8763, 2021.
- [60] C. Raffel, N. Shazeer, A. Roberts, K. Lee, S. Narang, M. Matena, Y. Zhou, W. Li, and P. J. Liu. Exploring the limits of transfer learning with a unified text-to-text Transformer. *J. Mach. Learn. Res.*, 21(140):1–67, 2020.
- [61] A. Ramesh, P. Dhariwal, A. Nichol, C. Chu, and M. Chen. Hierarchical text-conditional image generation with CLIP latents. *arXiv preprint arXiv:2204.06125*, 2022.
- [62] B. Recht, R. Roelofs, L. Schmidt, and V. Shankar. Do imagenet classifiers generalize to imagenet? In *Int. Conf. Mach. Learn.*, 2019.
- [63] R. Rombach, A. Blattmann, D. Lorenz, P. Esser, and B. Ommer. High-resolution image synthesis with latent diffusion models. In *IEEE Conf. Comput. Vis. Pattern Recog.*, pages 10684–10695, 2022.
- [64] O. Ronneberger, P. Fischer, and T. Brox. U-Net: Convolutional networks for biomedical image segmentation. In *Med. Image Comput. Computer-Assisted Interv.*, pages 234–241, 2015.
- [65] N. Ruiz, Y. Li, V. Jampani, Y. Pritch, M. Rubinstein, and K. Aberman. Dreambooth: Fine tuning text-to-image diffusion models for subject-driven generation. In *IEEE Conf. Comput. Vis. Pattern Recog.*, 2022.
- [66] R. Socher, A. Perelygin, J. Wu, J. Chuang, C. D. Manning, A. Ng, and C. Potts. Recursive deep models for semantic compositionality over a sentiment treebank. In *Conf. Empirical Methods NLP*, pages 1631–1642, 2013.

- [67] H. Song, D. Sun, S. Chun, V. Jampani, D. Han, B. Heo, W. Kim, and M.-H. Yang. ViDT: An efficient and effective fully Transformer-based object detector. In *Int. Conf. Learn. Represent.*, 2022.
- [68] Y.-L. Sung, J. Cho, and M. Bansal. LST: Ladder side-tuning for parameter and memory efficient transfer learning. In *Adv. Neural Inform. Process. Syst.*, 2022.
- [69] G. Van Horn, S. Branson, R. Farrell, S. Haber, J. Barry, P. Ipeirotis, P. Perona, and S. Belongie. Building a bird recognition app and large scale dataset with citizen scientists: The fine print in fine-grained dataset collection. In *IEEE Conf. Comput. Vis. Pattern Recog.*, pages 595–604, 2015.
- [70] A. Vaswani, N. Shazeer, N. Parmar, J. Uszkoreit, L. Jones, A. N. Gomez, Ł. Kaiser, and I. Polosukhin. Attention is all you need. In *Adv. Neural Inform. Process. Syst.*, volume 30, 2017.
- [71] B. S. Veeling, J. Linmans, J. Winkens, T. Cohen, and M. Welling. Rotation equivariant cnns for digital pathology. In *Med. Image Comput. Computer-Assisted Interv.*, 2018.
- [72] C. Wah, S. Branson, P. Welinder, P. Perona, and S. Belongie. The Caltech-UCSD Birds-200-2011 dataset. *California Institute of Technology*, 2011.
- [73] H. Wang, S. Ge, Z. C. Lipton, and E. P. Xing. Learning robust global representations by penalizing local predictive power. In *Adv. Neural Inform. Process. Syst.*, 2019.
- [74] W. Wang, E. Xie, X. Li, D.-P. Fan, K. Song, D. Liang, T. Lu, P. Luo, and L. Shao. Pyramid vision Transformer: A versatile backbone for dense prediction without convolutions. In *Int. Conf. Comput. Vis.*, pages 568–578, 2021.
- [75] W. Wang, H. Bao, L. Dong, J. Bjorck, Z. Peng, Q. Liu, K. Aggarwal, O. K. Mohammed, S. Singhal, S. Som, et al. Image as a foreign language: Beit pretraining for all vision and vision-language tasks. *arXiv preprint arXiv:2208.10442*, 2022.
- [76] Z. Wang, Z. Zhang, S. Ebrahimi, R. Sun, H. Zhang, C.-Y. Lee, X. Ren, G. Su, V. Perot, J. Dy, et al. DualPrompt: Complementary prompting for rehearsal-free continual learning. In *Eur. Conf. Comput. Vis.*, 2022.
- [77] A. Williams, N. Nangia, and S. Bowman. A broad-coverage challenge corpus for sentence understanding through inference. In *North Am. Chap. Assoc. Comput. Linguist.*, pages 1112–1122, 2018.
- [78] J. Xiao, J. Hays, K. A. Ehinger, A. Oliva, and A. Torralba. SUN database: Large-scale scene recognition from abbey to zoo. In *IEEE Conf. Comput. Vis. Pattern Recog.*, pages 3485–3492, 2010.
- [79] E. B. Zaken, S. Ravfogel, and Y. Goldberg. BitFit: Simple parameter-efficient fine-tuning for Transformer-based masked language-models. *Assoc. Comput. Linguist.*, 2021.
- [80] X. Zhai, J. Puigcerver, A. Kolesnikov, P. Ruysen, C. Riquelme, M. Lucic, J. Djolonga, A. S. Pinto, M. Neumann, A. Dosovitskiy, et al. A large-scale study of representation learning with the visual task adaptation benchmark. *arXiv preprint arXiv:1910.04867*, 2019.
- [81] X. Zhai, A. Kolesnikov, N. Houlsby, and L. Beyer. Scaling Vision Transformers. In *IEEE Conf. Comput. Vis. Pattern Recog.*, pages 12104–12113, 2022.
- [82] J. O. Zhang, A. Sax, A. Zamir, L. J. Guibas, and J. Malik. Side-Tuning: Network adaptation via additive side networks. In *Eur. Conf. Comput. Vis.*, 2019.
- [83] Y. Zhang, K. Zhou, and Z. Liu. Neural prompt search. *arXiv preprint arXiv:2206.04673*, 2022.
- [84] S. Zheng, J. Lu, H. Zhao, X. Zhu, Z. Luo, Y. Wang, Y. Fu, J. Feng, T. Xiang, P. H. Torr, and L. Zhang. Rethinking semantic segmentation from a sequence-to-sequence perspective with Transformers. In *IEEE Conf. Comput. Vis. Pattern Recog.*, 2021.
- [85] K. Zhou, J. Yang, C. C. Loy, and Z. Liu. Conditional prompt learning for vision-language models. In *IEEE Conf. Comput. Vis. Pattern Recog.*, pages 16816–16825, 2022.

In the appendix, we provide a detailed derivation process for turning existing PETL methods into our unbinding formulation (appendix A), demonstration of our unbinding formulation as a unified formulation for existing PETL methods (appendix B), more implementation details (appendix C) including the dataset used, architectures for discriminative and generative tasks, and hyperparameters used in training, additional results on discriminative tasks (appendix D) and generative tasks (appendix E).

A Detailed derivations

In this section, we provide the detailed deriving process for the existing prefix [41] and prompt [28] tuning to be turned into our unbinding formulation.

Prefix tuning [41]: The following is the detailed derivation of Eq. (3).

$$\begin{aligned}
\text{MHA}_{\text{pre}} &= \text{Attn}(\mathbf{x}\mathbf{W}_q, [\mathbf{K}_{\text{pre}}; \mathbf{x}\mathbf{W}_k], [\mathbf{V}_{\text{pre}}; \mathbf{x}\mathbf{W}_v]) \\
&= \text{softmax}(\mathbf{x}\mathbf{W}_q[\mathbf{K}_{\text{pre}}; \mathbf{x}\mathbf{W}_k]^\top) \begin{bmatrix} \mathbf{V}_{\text{pre}} \\ \mathbf{x}\mathbf{W}_v \end{bmatrix} \\
&= (1 - \lambda(\mathbf{x})) \text{softmax}(\mathbf{x}\mathbf{W}_q\mathbf{W}_k^\top \mathbf{x}^\top) \mathbf{x}\mathbf{W}_v + \lambda(\mathbf{x}) \text{softmax}(\mathbf{x}\mathbf{W}_q\mathbf{K}_{\text{pre}}^\top) \mathbf{V}_{\text{pre}} \quad (9) \\
&= (1 - \lambda(\mathbf{x})) \text{Attn}(\mathbf{x}\mathbf{W}_q, \mathbf{x}\mathbf{W}_k, \mathbf{x}\mathbf{W}_v) + \lambda(\mathbf{x}) \text{Attn}(\mathbf{x}\mathbf{W}_q, \mathbf{K}_{\text{pre}}, \mathbf{V}_{\text{pre}}) \\
&= (1 - \lambda(\mathbf{Q}, \mathbf{K}, \mathbf{K}_{\text{pre}})) \underbrace{\text{Attn}(\mathbf{Q}, \mathbf{K}, \mathbf{V})}_{\text{standard attention}} + \lambda(\mathbf{Q}, \mathbf{K}, \mathbf{K}_{\text{pre}}) \underbrace{\text{Attn}(\mathbf{Q}, \mathbf{K}_{\text{pre}}, \mathbf{V}_{\text{pre}})}_{\text{independent of } \mathbf{K}_{\text{pre}}, \mathbf{V}_{\text{pre}}}
\end{aligned}$$

where \mathbf{Q} , \mathbf{K} denote the original query and original key, \mathbf{K}_{pre} and \mathbf{V}_{pre} are prefix key tokens and prefix value tokens, and

$$\lambda(\mathbf{Q}, \mathbf{K}, \mathbf{K}_{\text{pre}}) = \frac{\sum_i \exp(\mathbf{Q}\mathbf{K}_{\text{pre}}^\top)_i}{\sum_i \exp(\mathbf{Q}\mathbf{K}^\top)_i + \sum_j \exp(\mathbf{Q}\mathbf{K}_{\text{pre}}^\top)_j}, \quad (10)$$

Prompt tuning [28]: The following is the detailed derivation of Eq. (5).

$$\begin{aligned}
\text{MHA}_{\text{pro}} &= \text{Attn}([\mathbf{x}; \mathbf{x}_{\text{pro}}]\mathbf{W}_q, [\mathbf{x}; \mathbf{x}_{\text{pro}}]\mathbf{W}_k, [\mathbf{x}; \mathbf{x}_{\text{pro}}]\mathbf{W}_v) \\
&= \text{concat} \left(\text{softmax}(\mathbf{x}\mathbf{W}_q[\mathbf{x}\mathbf{W}_k; \mathbf{x}_{\text{pro}}\mathbf{W}_k]^\top) \begin{bmatrix} \mathbf{x}\mathbf{W}_v \\ \mathbf{x}_{\text{pro}}\mathbf{W}_v \end{bmatrix}, \right. \\
&\quad \left. \text{softmax}(\mathbf{x}_{\text{pro}}\mathbf{W}_q[\mathbf{x}\mathbf{W}_k; \mathbf{x}_{\text{pro}}\mathbf{W}_k]^\top) \begin{bmatrix} \mathbf{x}\mathbf{W}_v \\ \mathbf{x}_{\text{pro}}\mathbf{W}_v \end{bmatrix} \right) \\
&= \text{concat}((1 - \lambda(\mathbf{Q}, \mathbf{K}, \mathbf{K}_{\text{pro}})) \text{Attn}(\mathbf{Q}, \mathbf{K}, \mathbf{V}) + \lambda(\mathbf{Q}, \mathbf{K}, \mathbf{K}_{\text{pro}}) \text{Attn}(\mathbf{Q}, \mathbf{K}_{\text{pro}}, \mathbf{V}_{\text{pro}}), \\
&\quad (1 - \beta(\mathbf{Q}_{\text{pro}}, \mathbf{K}_{\text{pro}}, \mathbf{K})) \text{Attn}(\mathbf{Q}_{\text{pro}}, \mathbf{K}_{\text{pro}}, \mathbf{V}_{\text{pro}}) \\
&\quad + \beta(\mathbf{Q}_{\text{pro}}, \mathbf{K}_{\text{pro}}, \mathbf{K}) \text{Attn}(\mathbf{Q}_{\text{pro}}, \mathbf{K}, \mathbf{V})) \quad (11)
\end{aligned}$$

where \mathbf{K}_{pro} and \mathbf{V}_{pro} are prompt key tokens and prompt value tokens, and

$$\lambda(\mathbf{Q}, \mathbf{K}, \mathbf{K}_{\text{pro}}) = \frac{\sum_i \exp(\mathbf{Q}\mathbf{K}_{\text{pro}}^\top)_i}{\sum_i \exp(\mathbf{Q}\mathbf{K}^\top)_i + \sum_j \exp(\mathbf{Q}\mathbf{K}_{\text{pro}}^\top)_j}, \quad (12)$$

$$\beta(\mathbf{Q}_{\text{pro}}, \mathbf{K}_{\text{pro}}, \mathbf{K}) = \frac{\sum_i \exp(\mathbf{Q}_{\text{pro}}\mathbf{K}^\top)_i}{\sum_i \exp(\mathbf{Q}_{\text{pro}}\mathbf{K}_{\text{pro}}^\top)_i + \sum_j \exp(\mathbf{Q}_{\text{pro}}\mathbf{K}^\top)_j}, \quad (13)$$

B Unified formulation

From Eq. (7), we derive a unified formulation for existing PETL methods, which is the combination of the frozen pre-trained operation (OP) and the tuner with learnable parameters (Res-Tuner). The following is the detailed instantiation of this unified formulation (as in Tab. 7). Thanks to the form of unbinding, tuners can be treated as individual and flexibly combined. Our framework can effectively encompass existing tuning methods in a residual form and is not limited to the OP and Res-Tuner mentioned in our work. For example, for MAM-Adapter, we are free to attach Res-Prefix and Res-Adapter to MHA and FFN modules, respectively. In particular, when new PETL methods are proposed, they can be quickly applied (abbreviated as New-Tuning), and different methods can be arbitrarily combined (abbreviated as Mix-Tuning).

Table 7: The combination of Res-Tuning.

Method	OP	Res-Tuner
Adapter [25]	FFN	Res-Adapter
Prefix [41]	MHA	Res-Prefix
Prompt [28]	MHA	Res-Prompt
LoRA [27]	Weight	MLP
BitFit [79]	Bias	Parameter
AdaptFormer [7]	FFN	Res-Adapter
MAM-Adapter [19]	MHA + FFN	Res-Prefix + Res-Adapter
Side-Tuning [82]	All blocks	Side model
LST [68]	Block	ViT
New-Tuning	Any where	New-Tuner
Mix-Tuning	Any combination	Any combination

C Implementation details

C.1 Dataset description

In Tab. 8 and Tab. 9, we list the description of each dataset in our experiments, which includes the number of classes and the amount of images in training set and test set for discriminative and generative tasks, respectively.

Table 8: Datasets used for generative tasks. * denotes only part of the data is used.

Dataset	Description	Classes	Train		Test	
			image	prompt	image	prompt
<i>Common Objects in Context (COCO)</i>						
COCO2017 Captions	common objects	-	118287	591753	5000	25014
<i>Fine-grained Image Generation</i>						
Aircraft [51]*	Fine-grained aircraft	100	3334	-	3333	-
Food-101 [4]*	Fine-grained food	101	75750	-	25250	-
NABirds [69]*	Fine-grained bird	555	23929	-	24633	-
Stanford Cars [15]*	Fine-grained car	196	8144	-	8144	-
Stanford Dogs [34]*	Fine-grained dog	120	12000	-	8580	-
SUN397 [78]*	Fine-grained scene	397	76044	-	16295	-

Table 9: Datasets used for discriminative tasks.

Dataset	Description	Classes	Train	Test
<i>General Image Classification</i>				
CIFAR-100 [35]	General	100	50000	10000
<i>Fine-grained Visual Classification (FGVC)</i>				
CUB-200-2011 [72]	Bird	200	5994	5794
NABirds [69]	Bird	555	23929	24633
Oxford Flowers [55]	Flower	102	1020	6149
Stanford Cars [15]	Car	196	8144	8041
Stanford Dogs [34]	Dog	120	12000	8580
<i>Visual Task Adaptation Benchmark (VTAB-1K)</i>				
CIFAR-100 [35]	Natural	100	1000	10000
Caltech101 [38]		102		6084
DTD [9]		47		1880
Flower102 [55]		102		6149
Pets [56]		37		3669
SVHN [54]		10		26032
SUN397 [78]		397		21750
Camelyon [71]		2		32768
EuroSAT [22]	Specialized	10	1000	5400
Resisc45 [8]		45		6300
Retinopathy [18]		5		42670
Clevr-Count [30]		8		15000
Clevr-Dist [30]	Structured	6	1000	15000
DMLab [3]		6		22735
KITTI-Dist [16]		4		711
dSpr-Loc [52]		16		73728
dSpr-Ori [52]		16		73728
sNORB-Azim [36]		18		12150
sNORB-Ele [36]		9		12150
<i>Few-Shot Learning</i>				
FGVC-Aircraft [51]	Aircraft	100	(1/2/4/8/16) * class	3333
Food-101 [4]	Food	101	(1/2/4/8/16) * class	30300
Oxford Flowers [55]	Flower	102	(1/2/4/8/16) * class	2463
Oxford Pets [56]	Pet	37	(1/2/4/8/16) * class	3669
Stanford Cars [15]	Car	196	(1/2/4/8/16) * class	8041
<i>Domain Generalization</i>				
ImageNet-1K [11]	General	1000	16 * class	50000
ImageNet-V2 [62]	General	1000	/	10000
ImageNet-Sketch [73]	General	1000	/	50889
ImageNet-A [24]	General	200	/	7500
ImageNet-R [23]	General	200	/	30000

C.2 Architectures design

We show the complete Res-Tuning-Bypass structural design according to the different task frameworks. For discriminative tasks, we design based on the architecture of Vision Transformers [13], mainly based on main blocks and unbound bypass (as in Fig. 8). For generative tasks, we design based on the stable diffusion [63] framework and innovatively apply Res-Tuner to U-Net [64] structure (as in Fig. 9). We attach Res-Tuner to the U-Net intermediate module and decoder module for more efficient training.

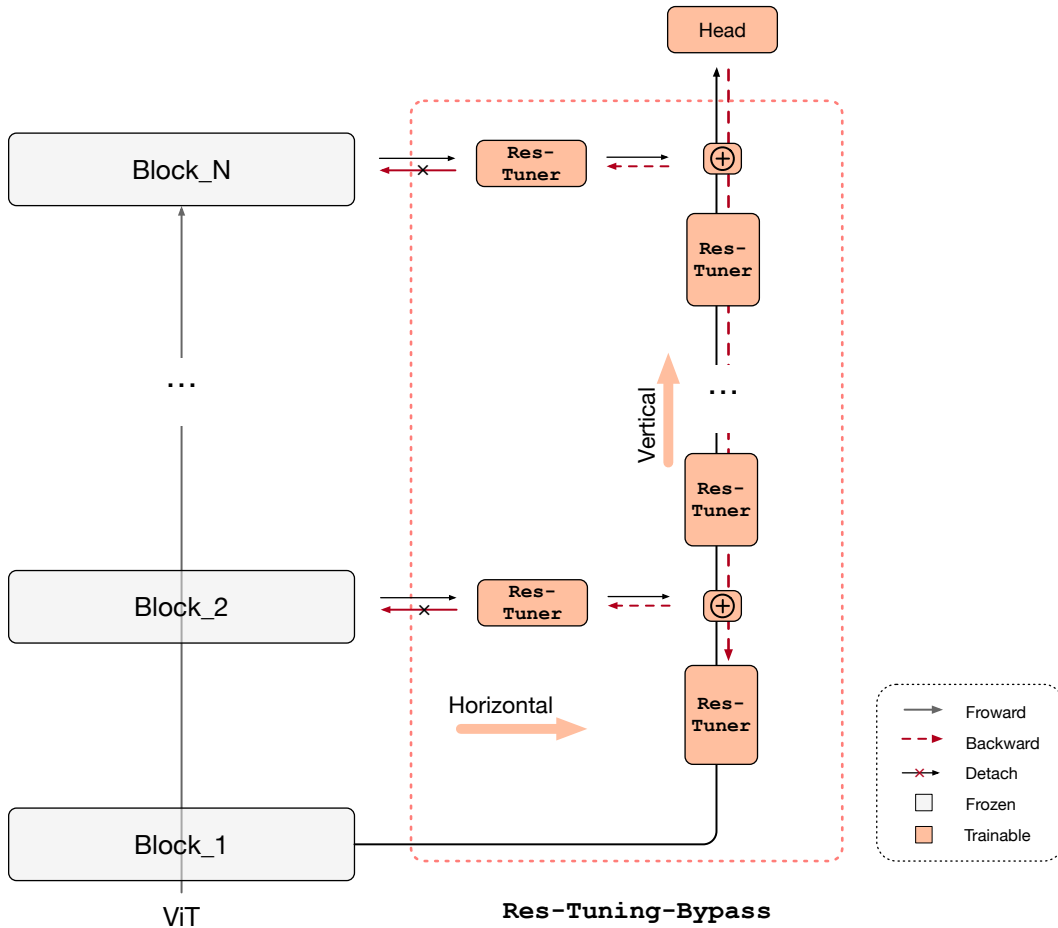


Figure 8: Architecture design for discriminative tasks.

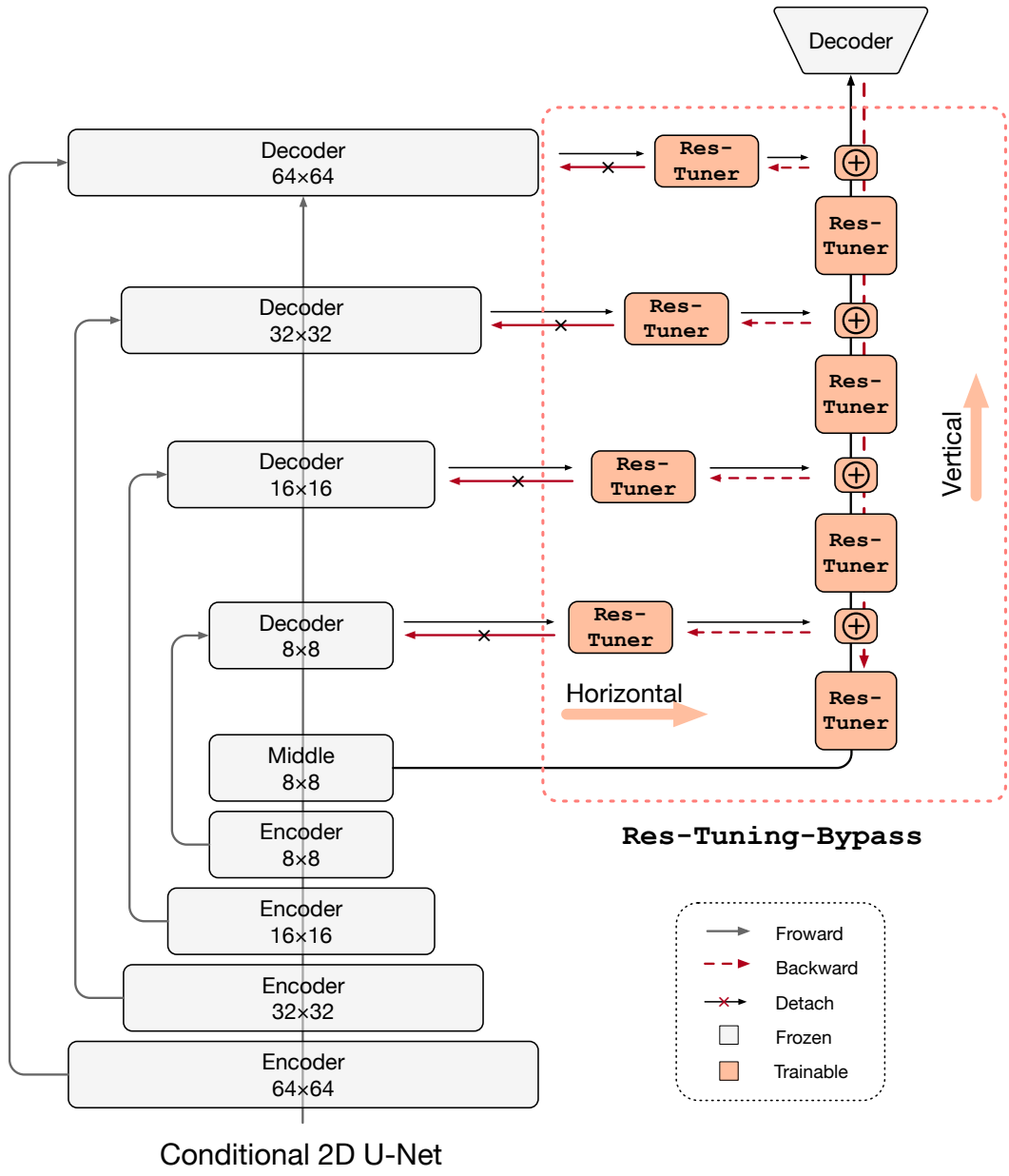


Figure 9: Architecture design for generative tasks.

C.3 Hyperparameters

We list all the hyperparameters for discriminative (see in Tab. 10) and generative (see in Tab. 11) tasks.

Table 10: Hyperparameter selection for discriminative tasks.

Config	Value
Batch size	32
Optimizer	AdamW [50]
Weight decay	0.05
Base learning rate range	{0.05, 0.01, 0.005, 0.001}
Learning rate schedule	Cosine decay
Training epochs range	{50, 100}
Warmup epochs	10
Augmentation	RandomResizedCrop, RandomHorizontalFlip
OP	MHA [70] FFN [70] Block [70]
Res-Tuner	Res-Adapter Res-Prefix Res-Prompt
Architecture	ViT/B-16 [13] ViT/L-14 [13]
Pre-trained	ImageNet-21K [11] CLIP [59]
Device	A100 × 1

Table 11: Hyperparameter selection for generative tasks.

Config	Value
Batch size	8
Optimizer	AdamW [50]
Base learning rate	1e-4
Learning rate schedule	Constant
Training epochs	10
Augmentation	CenterCrop, RandomHorizontalFlip
Resolution	512 × 512
Sampler	PLMS [44]
Guidance	3.0
OP	MHA [70] FFN [70] Block [70] Conditional 2D U-Net [64]
Res-Tuner	Res-Adapter Res-Prefix Res-Prompt
Architecture	Stable Diffusion [63]
Pre-trained	Stable Diffusion v1.5 [63] CLIP [59]
Device	A100 × 8
Library	Diffusers ²

²<https://github.com/huggingface/diffusers>

D Additional experiments on discriminative tasks

D.1 Comparisons on FGVC datasets

We compare the transfer ability of our Res-Tuning framework with different existing approaches for parameter- and memory-efficient transfer learning on FGVC datasets. As shown in Tab. 12, our Res-Tuning outperforms other tuning methods on the average accuracy of five FGVC datasets. For memory-efficient methods, Res-Tuning-Bypass achieves a 2.89% improvement compared to LST [68] with less memory consumption.

Table 12: **Performance and efficiency comparison** on FGVC. † denotes our own implementation.

Method \ Datasets	CUB-200-2011	NABirds	Oxford Flowers	Stanford Cars	Stanford Dogs	Mean	Param. (M)	Mem. (GB)
Full	87.3	82.7	98.8	84.5	89.4	88.54	85.98	9.40
Linear	85.3	75.9	97.9	51.3	86.2	79.32	0.18	3.09
<i>Parameter-efficient tuning methods</i>								
Adapter [25]	87.3	84.3	98.4	68.4	88.8	85.46	1.96	6.55
Prefix† [41]	85.4	78.8	99.2	76.4	89.5	85.86	0.36	6.60
VPT-Shallow [28]	86.7	78.8	98.4	68.7	90.7	84.62	0.25	8.14
VPT-Deep [28]	88.5	84.2	99.0	83.6	90.2	89.11	0.85	8.16
LoRA† [27]	86.0	80.2	99.2	85.2	88.6	87.84	0.55	6.78
Convpass† [29]	86.9	81.4	99.3	85.7	89.9	88.66	0.51	7.44
SSF [42]	89.5	85.7	99.6	89.2	89.6	90.72	0.39	7.47
Res-Tuning	89.66	85.87	99.45	87.58	92.21	90.95	0.68	8.98
<i>Memory-efficient tuning methods</i>								
Side-Tuning [82]	84.7	75.8	96.9	48.6	85.8	78.35	9.73	3.48
LST† [68]	82.98	76.11	98.83	78.46	87.89	84.85	1.04	5.28
Res-Tuning-Bypass	88.75	83.00	99.61	75.41	92.40	87.83	0.56	4.73

D.2 More ablation studies

Varying the length of dimensions. The length of dimensions represents the hidden dimension for Res-Adapter and the number of tokens of Res-Prompt and Res-Prefix. Altering the length of dimensions affects performances, the number of parameters, and memory consumption simultaneously (see in Tab. 13). By default, we use the length that balances the number of parameters and memory, although there is a slight increase as the length grows to a certain extent.

Table 13: Ablation studies on the length of dimension for Res-Tuning on CIFAR-100. Default setting is marked in gray.

Dim	Res-Tuning			Res-Tuning-Bypass		
	Acc.	Param.	Mem.	Acc.	Param.	Mem.
5	93.03	0.30M	6.84G	89.16	0.37M	4.65G
10	93.25	0.48M	6.85G	89.33	0.46M	4.72G
20	92.98	0.85M	6.87G	89.28	0.64M	4.83G
50	92.69	1.96M	6.90G	89.22	1.19M	5.08G
100	92.48	3.80M	6.96G	89.52	2.11M	5.68G

Different number of block layers. Based on the ViT/B-16 structure, we change the number of block layers in two ways: (i) increase from head to toe gradually (see in Tab. 14), (ii) discard several intermediate layers (see in Tab. 15), and evaluate the impact of using a different number of layers. It can be seen that the best performance can be achieved by using the full number of layers, but it requires the use of relatively more parameters and memory.

Table 14: Ablation studies on the tuning block layers for Res-Tuning on CIFAR-100. The right arrow denotes use the number of all layers from left to right. Default setting is marked in gray.

Blocks	Res-Tuning			Res-Tuning-Bypass		
	Acc.	Param.	Mem.	Acc.	Param.	Mem.
1 → 1	92.23	0.11M	6.43G	88.50	0.11M	3.58M
1 → 3	92.78	0.18M	6.52G	88.60	0.17M	3.73G
1 → 6	92.93	0.28M	6.64G	89.05	0.27M	4.09G
1 → 9	93.17	0.38M	6.84G	89.32	0.36M	4.53G
1 → 12	93.25	0.48M	6.85G	89.33	0.46M	4.72G

Table 15: Ablation studies on the drop block layers for Res-Tuning on CIFAR-100. Inside the braces indicate the layer number that is discarded. The default setting is marked in gray.

Drop block layers	Res-Tuning			Res-Tuning-Bypass		
	Acc.	Param.	Mem.	Acc.	Param.	Mem.
{}	93.25	0.48M	6.85G	89.33	0.46M	4.72G
{3, 6, 9}	92.88	0.38M	6.73G	89.30	0.36M	4.36G
{2, 3, 5, 7, 9, 11}	92.96	0.28M	6.68G	88.89	0.27M	3.96G
{2, 3, 4, 5, 6, 8, 9, 10, 11}	92.71	0.18M	6.56G	88.79	0.17M	3.65G
{1, 2, 3, 4, 5, 6, 7, 8, 9, 10, 11}	87.77	0.11M	3.31G	88.49	0.11M	3.48G

Different CNN backbones. We present the results for ConvNeXt [49] and ResNet-101 [20] pre-trained on ImageNet-21K in Tab. 16. We observe that two convolutional models have different characteristics, where the performance variation of ConvNeXt is small and that of ResNet is large. In terms of the effectiveness of Res-Tuning-Bypass, it is observed that it outperforms the fully-finetuned version of ConvNeXt and notably improves the performance of linear probing for ResNet.

Table 16: Ablation studies on the CNN-based backbones on CIFAR-100.

Method	ConvNext			ResNet-101		
	Acc.	Param.	Mem.	Acc.	Param.	Mem.
Full	90.15	87.67	11.16	77.40	42.70	7.30
Linear	90.06	0.11	3.36	54.96	0.20	2.83
Res-Tuning	90.86	0.87	9.45	86.80	0.92	7.20
Res-Tuning-Bypass	90.51	1.13	3.63	72.27	3.63	4.05

Experiments on NLP downstream task. We also conduct experiments on downstream tasks beyond vision. For NLP, we perform experiments on the SST2 [66] and MNLI [77] datasets for text classification tasks. It is observed that the performance of our Res-Tuning framework is on par with or better than MAM-Adapter [19] in text classification, with slightly longer training time but lower memory consumption. Our Res-Tuning-Bypass significantly reduces the training time and memory consumption and achieves a mildly lower performance.

Table 17: Performance comparison on text classification task.

Method	SST2		MNLI		Train Param.	Test Param.	Mem.
	Acc.	Train Time	Acc.	Train Time			
MAM Adapter [19]	94.2	7.2	87.4	41.4	46.78 (37.4%)	0.61 (0.5%)	22.4G
Res-Tuning	94.56	7.9	87.45	47.3	0.97 (0.77%)	0.97 (0.77%)	19.3G
Res-Tuning-Bypass	92.94	4.2	82.01	24.2	0.98 (0.78%)	0.98 (0.78%)	4.3G

E Additional Experiments on generative tasks

E.1 More visualizations on COCO

We present more visualization results, comparing real images, stable diffusion [63] (SD) v1.5, fully fine-tuning, LoRA [27], Res-Tuning and Res-Tuning-Bypass in Fig. 10 and more detailed generated image in Fig. 11. Specifically, the text conditions of text-to-image task are sampled from COCO Captions. To better demonstrate the advantages of our approach in understanding the concepts of text, the main elements are marked in blue, and the main modifiers or prepositions are marked in green.

E.2 More visualizations on fine-grained datasets

We present more visualization results on fine-grained datasets (see in Fig. 12, Fig. 13, and Fig. 14), including NABirds [69], Stanford Dogs [34], Stanford Cars [15], Aircraft [51], SUN397 [78] and Food-101 [4].

F Limitations and Societal Impacts

This work is a tuning paradigm that is fine-tuned based on the pre-trained foundation models while freezing the backbone network, so its transfer ability depends to a large extent on the performance of the upstream model. However, when the upstream pre-training model contains illegal content training, it will also lead to the illegal use of tuning methods.

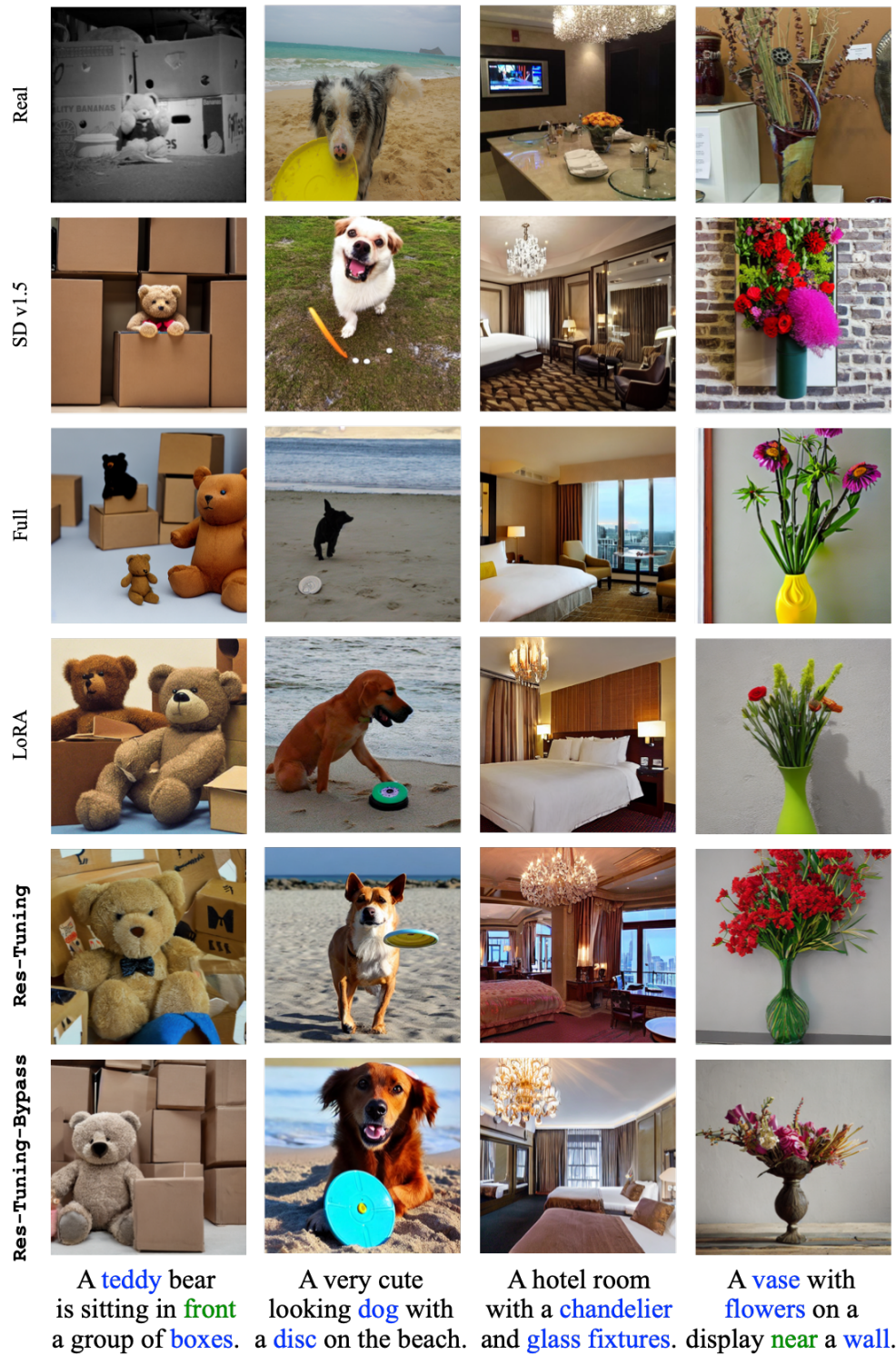


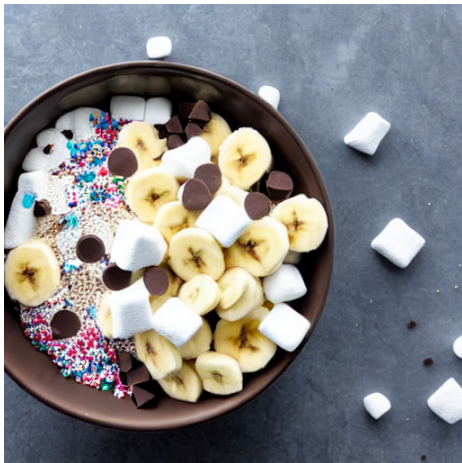
Figure 10: Qualitative results of existing tuning strategies and our Res-Tuning on COCO2017 validation set.



A landscape with water, a boat, trees and mountains.



Two elephants standing next to each other in a field.



Bananas, marshmallows, chocolate chips and sprinkles in a bowl.



A single white rose in a glass vase.



The rain is pouring on the white car on the street.



A close up of glazed donuts that are plain or with chocolate.

Figure 11: Visualization of our Res-Tuning on COCO2017 validation set.

NABirds

Stanford Dogs



(a) Res-Tuning



(b) Res-Tuning-Bypass

Figure 12: Visualization of our Res-Tuning on NABirds and Stanford Dogs.

Stanford Cars

Aircraft



(a) Res-Tuning

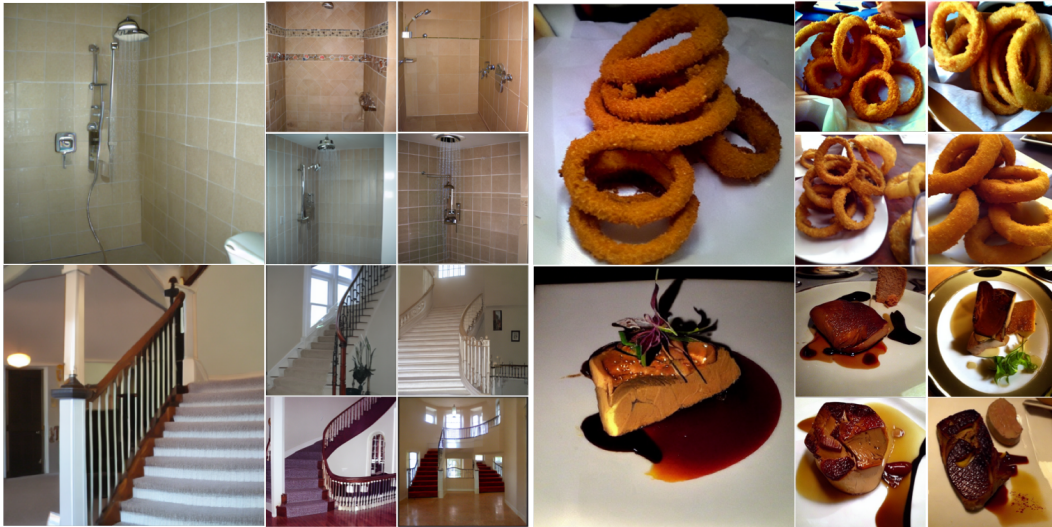


(b) Res-Tuning-Bypass

Figure 13: Visualization of Res-Tuning on Stanford Cars and Aircraft.

SUN397

Food-101



(a) Res-Tuning



(b) Res-Tuning-Bypass

Figure 14: Visualization of Res-Tuning on SUN397 and Food-101.